US Army Corps
of Engineers®
Engineer Research and
Development Center

Geotechnical and Structures Laboratory

The Behaviour of Near-Surface Soils Through Ultrasonic Near-Surface Inundation Testing

Oliver-Denzil S. Taylor, Amy L. Cunningham,
Robert E. Walker, Mihan H. McKenna, Kathryn E. Martin,
and Pamela G. Kinnebrew

August 2021

The U.S. Army Engineer Research and Development Center (ERDC) solves the nation's toughest engineering and environmental challenges. ERDC develops innovative solutions in civil and military engineering, geospatial sciences, water resources, and environmental sciences for the Army, the Department of Defense, civilian agencies, and our nation's public good. Find out more at www.erdc.usace.army.mil.

To search for other technical reports published by ERDC, visit the ERDC online library at https://erdclibrary.on.worldcat.org/discovery.

The Behaviour of Near-Surface Soils Through Ultrasonic Near-Surface Inundation Testing

Oliver-Denzil S. Taylor, Amy L. Cunningham, Robert E. Walker, Mihan H. McKenna, Kathryn E. Martin, and Pamela G. Kinnebrew

Geotechnical and Structures Laboratory
U.S. Army Engineer Research and Development Center
3909 Halls Ferry Road
Vicksburg, MS 39180

Final report

Preface

The behaviour of near-surface soils through ultrasonic near-surface inundation testing

ABSTRACT

Seismometers installed within the upper metre of the subsurface can experience significant variability in signal propagation and attenuation properties of observed arrivals due to meteorological events. For example, during rain events, both the time and frequency representations of observed seismic waveforms can be significantly altered, complicating potential automatic signal processing efforts. Historically, a lack of laboratory equipment to explicitly investigate the effects of active inundation on seismic wave properties in the near surface prevented recreation of the observed phenomena in a controlled environment. Presented herein is a new flow chamber designed specifically for near-surface seismic wave/fluid flow interaction phenomenology research, the ultrasonic near-surface inundation testing device and new v_p-saturation and v_s-saturation relationships due to the effects of matric suction on the soil fabric.

1 INTRODUCTION

Seismic arrays are precisely located collections of seismometers utilized to monitor subsurface and near-surface events, spanning a variety of technologies from permanently emplaced borehole seismometer networks to monitor earthquakes (Chapman 2013), to mobile and temporarily deployed oil and gas land-streamer geophone survey rigs (Tsoflias *et al.* 2006). In each case, there is a trade-off between ideal location, such as quiet and isolated basement rock emplacement for global seismic earthquake monitoring, and ideal conditions, like those found in targeted near-surface seismic surveys that occur only at discrete points in time under non-variable meteorological conditions. Through careful analysis, these seismic arrays can forensically investigate events of interest, such as discrimination of nuclear and chemical explosions (Stump,

Pearson and Reinke 1999), pipeline explosions (Koper, Wallace and Aster 2003) and even military events (Bonner *et al.* 2013). Both ideal location and ideal condition seismic array techniques are able to effectively reconstruct source properties such as duration, spatial length, strength or dominant period and yield, because receiver side effects are able to be properly quantified for each deployment. This assessment critically relies on behavioural knowledge of the rock (deep borehole placement) or soil (shallow, temporary geophone deployments) through which the seismic energy will propagate. Unlike the traditional seismic array deployments discussed above, semi-permanent 'operational' seismic arrays deployed for extended periods of time are often situated within near-surface soils, not hard rock or other more competent material, and are therefore subject to the meteorologically sensitive behaviour low-confinement soils can exhibit (Taylor *et al.* 2014).

Taylor *et al.* (2014) observed that near-surface post-rain signals are amplified up to 14.7-fold over the pre-rain

signals in *in situ* sand testing, with significant shifts in spectral content and shear wave arrival times at low to negligible confining stresses. Moreover, Taylor *et al.* (2014) observed a significant shift in the shear wave velocities along all principle axes, wherein the soil fabric went from an anisotropic state to an isotropic state signifying a complex realignment of granular stresses. Fratta *et al.* (2005) illustrated the need for accurate new v_p-saturation and v_s-saturation relationships for validation of empirical and semi-empirical stiffness models used to derived elastic moduli. Therefore, understanding this relatively unconfined behaviour along with highly accurate elastic moduli becomes paramount in order to perform any detection, classification or localization of seismic sources over a broad spectrum of meteorological conditions.

Presented herein is a new flow chamber designed specifically for near surface seismic wave/fluid flow interaction phenomenology research, the ultrasonic near-surface inundation testing device and new v_p-saturation and v_s-saturation relationships due to the effects of matric suction on the soil fabric.

2 THEORY

2.1 Near-surface soil behaviour

The behaviour of dry, moist and saturated soils has been studied for over a century without adequately investigating the behaviour associated with transient saturation in upper the near surface, including the effects of rapid meteorological changes, dynamic fluid flow and variability of saturation on shallow seismic sensors. Though the inter-particle stresses in the top metre of the earth can have a significant effect on the shear modulus of the soil and consequently the wave velocities (Hassanizadeh, Celia and Dahle 2002; Lu and Sabatier 2009; Shen *et al.* 2016), the large variability in the pre- and post-rain waves, observed by Taylor *et al.* (2014), is not explained by simply accounting for microscopic inter-particle stresses at variable saturations (e.g. unsaturated soil mechanics as described by Bishop and Blight 1963; Lu, Godt and Wu 2010; Fredlund, Rahardjo and Fredlund 2012; and others), nor is it explained by accounting for seepage forces in Biot–Gassmann theory (Gassmann 1951; Biot 1956). For example, high-resolution shallow seismic reflection and refraction studies on tidal saturation infer changes in density from Biot–Gassmann theory wherein the shear modulus and the bulk modulus are assumed constant or nearly constant within the partially saturated range (Bachrach and Nur 1998a,b). Additionally in these studies, the measured volumetric water contents versus those derived from wave speeds show

significant variability wherein the derived velocities are higher than those measured *in situ* (Bachrach and Nur 1998a,b). This observed wave speed variability can lead to classification and signal identification errors in shallow (<1 m burial depth) semi-permanent 'operational' seismic arrays deployed for extended periods of time.

Many near-surface seismic velocity studies (e.g. Bachrach *et al.* 2000; Barriere *et al.* 2012) inundate the soil through groundwater table rise, which fails to replicate the dynamic inundation of the ground surface from a brief rain event, as observed by Taylor *et al.* (2014). Moreover, Taylor *et al.* (2014, 2019) show the potential for shear modulus and stress-strain behaviour variability as a function of gravimetric water content counter to the assumption of Biot–Gassmann theory, the refraction models assumptions by Bachrach and Nur (1998a,b), and other research wherein a single soil behaviour, e.g. poro-visco-elastic behaviour, or fixed value moduli are assumed (Bachrach, Dvorkin and Nur 2000; Barriere *et al.* 2012). The inclusion of suction for the determination of shear strength in unsaturated soil mechanics (e.g. Vanapalli *et al.* 1996; Lu *et al.* 2010; Han and Vanapalli 2016) do not accurately represent the changes in strength and matrix behaviour of sands under low confining pressures (Taylor *et al.* 2019). Therefore, the phenomenology observed by Taylor *et al.* (2014) must be a function of a physical behavioural process within the soil that is currently unaccounted for in prevailing theory (Taylor *et al.* 2019).

Recent research at the U.S. Army Engineer Research and Development Center has demonstrated that as confinement decreases, the soil does not act as a continuum; neither finite nor discrete element modelling can simulate the physical behaviour (Taylor *et al.* 2014; Song *et al.* 2017; Taylor *et al.* 2019). Moreover, current signal processing techniques do not account for soil fabric variability from wetting/drying hysteresis. Historically, the data used to produce the constitutive equations that found the basis of near-surface models are not representative of true low confinement regimes, in large part due to the dependency of these data on inferences from data collected with higher confinement laboratory testing equipment (Houston, Houston and Spadola 1988; Sture *et al.* 1998; Cho, Dodds and Santamarina 2006; Lu *et al.* 2010; Han and Vanapalli 2016; Taylor *et al.* 2019).

2.2 Laboratory testing for low confinement soils

Typical geotechnical laboratory testing equipment, for example triaxial, simple shear, resonant column, ring shear and soil-water retention curve devices, ultrasonic testing, etc., require

some degree of confinement, for example latex membranes and seating loads, to maintain sample stability and system-soil connectivity prior to testing. This requirement inevitably results in a condition that does not represent the upper 1 m of the subsurface profile, as no atmospheric elastic free-surface boundary exists within the experiment set-up. For example, a typical triaxial test will have a significant total stress confining pressure, σ_3, of approximately 100 kPa, and then an internal pore space pressure is then applied to create an effective stress condition of low confinement (e.g. 90 kPa pore pressure can be applied to a specimen confined at 100 kPa to achieve an effective stress condition of 10 kPa). Such pressures do not exist for natural surficial soils; therefore, the resulting laboratory data may not be representative of the actual granular matrix stress states (Cho and Santamarina 2001; Santamarina 2001; Taylor *et al.* 2014; Taylor *et al.* 2019). Recent research showed this to be the case through testing on unsupported columns of sand and low confinement resonant column testing (Taylor and Winters 2017; Taylor *et al.* 2019).

In addition to the testing apparatus, the method and repeatability of the sample preparation plays a significant factor in the potential range of acoustic propagation values and quantification of the initial and subsequent soil structure and behaviour (Oelze, O'Brien and Darmody 2002; Taylor *et al.* 2017).

2.3 Field experimentation of near-surface soils

Near-surface seismic research requires the generation of short, repeatable, broadband source signatures constant in spectral content such that variations in the received signal can be attributed solely to geophysical, geological and geotechnical phenomenology (Crane, Lorenzo and Harris 2013). However, field testing has been conducted using a variety of different sources at varying degrees of success (Jolly 1956; Miller *et al.* 1986, 1992; Hasbrouck 1991; Bachrach and Nur 1998a,b; Lu and Sabatier 2009; Yordkayhun *et al.* 2009; Crane *et al.* 2013; Bergamo *et al.* 2016a,b). Field testing is a valuable dataset especially for model validation and its use and importance should not be understated. However, *in situ* subsurface and soil particle heterogeneity is often generalized during data analysis. Testing results are thus site specific, which can make definitive statements about the cause of observational anomalies difficult without supporting laboratory data. In cases where experimentation is conducted on engineered soils under field conditions, for example Lu and Sabatier (2009), the repeatability of the soil preparation has influence on the

experimental data as observed in more controlled laboratory environments (Taylor *et al.* 2017).

3 MATERIALS AND METHODS

3.1 Ultrasonic near-surface inundation testing device

To experimentally replicate and understand these effects in a controlled environment, a new laboratory testing apparatus –the ultrasonic near-surface inundation testing (UNIT) device – was designed specifically for the low confining stress, near-surface environment (Taylor and Martin 2017). The design criterion of the UNIT device is that it must replicate near-surface conditions while providing a reliable means to extract soil fabric behaviour under static and dynamic influxes of moisture. The influx of moisture must be representative of various quantities of rainfall and of small stresses such that particle reorientation does not occur in the case of static exchange of air/fluid volumes. An atmospheric, elastic, free-surface air/soil interface that allows for the development of uninhibited soil swell characteristics is essential for near-surface investigations. Further, the shape, materials and size of the device must be sufficient to ensure that wave reflectance and the artificial transmission of the source signal around the outside of the cell chamber are effectively eliminated. All water used within the UNIT device must be initially purified, distilled and de-aired to remove the potential of chemical contaminants that could introduce an artificial bonding of soil particles.

The UNIT device, Fig. 1, is comprised of a soil cell, precipitation tank, reservoir tank and recirculating pump. The recirculating pump allows for a continuous controlled meteorological event that minimizes the surface impact of water droplets. For most geotechnical testing, water droplet impacts are negligible but for the small stress and strain conditions affecting granular re-orientation at the air/soil interface, not mitigating the surface impact can present an 'artefact' of the experimental setup and not actual phenomena. The top plate of the soil cell includes a pressure equalization port, which keeps the sample chamber at atmospheric pressure during testing. The UNIT, with a 15 cm × 15 cm × 15 cm interior dimension, has horizontal and vertical bender ports to measure seismic wave propagation perpendicular to, in-flow, and against the direction of fluid flow. The bender elements consist of a paired piezoelectric compressional (p-wave) and shear (s-wave) wave transducers that are 10-kHz, 14-volt sine wave drivers manufactured by GDS Instuments, Inc. London, United Kingdom. The bender elements can be arranged in
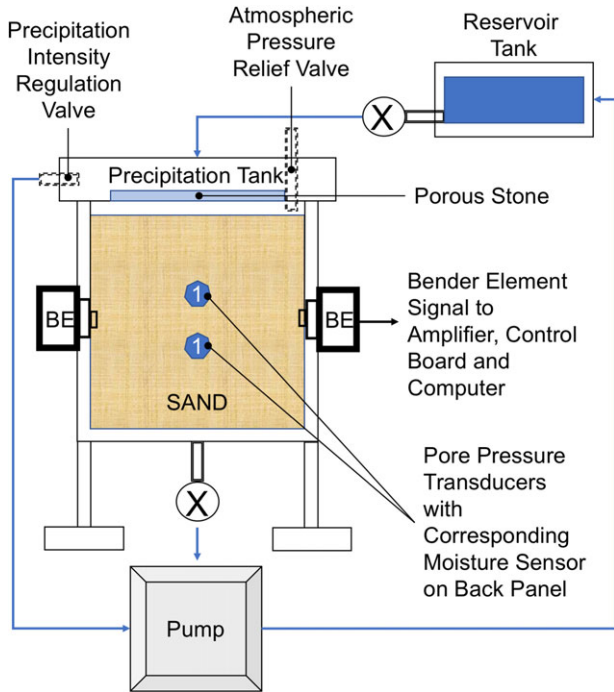
Figure 1 UNIT device schematic for this study. Bender elements are shown for radial motion comparison with field data (after Taylor and Martin 2017).

parallel or perpendicular orientation, depending on desired wave motion, Fig. 2. A series of resistivity posts or a moisture sensor is used to confirm the degree of saturation within the soil sample. Two piezometers are stacked vertically on the side of the sample chamber opposite moisture sensors to measure fluid pressures above and below the horizontal propagation pathway. Prior to the sample preparation, the outlet ball valve in the base plate is set to the desired drainage condition, ranging from free-draining to impermeable, and the head tank overflow outlet is set for a desired meteorological condition.

3.2 Controlled sample preparation

As sample preparation has a critical influence on the experimental limitations and data output, samples were prepared using an energy-based compaction method to ensure a repeatable initial soil fabric (Taylor *et al.* 2017). For laboratory reconstitution of a soil, there are three components that can be controlled; (a) the granular material, to include minerology, shape, particle distribution and mass; (b) the pore fluid, to include chemical composition, temperature and mass; and (c) the energy applied to the soil–water mixture, to include the method, quantity and uniformity of the application. The

characteristics of the resulting specimen, for example void ratio, fabric, permeability, compressibility, behaviour, etc., are a by-product that can be readily reproduced between samples (Taylor *et al.* 2017). To reduce epistemic uncertainty from sample preparation, samples exceeding a 2% differential from targeted water content or volume were discarded.

For experimental validation, all samples were reconstituted, using the Taylor *et al.* (2017) protocol at a remoulding saturation of 24% using a compaction energy of 600 kJ/m³, to a comparable soil fabric to the *in situ* field conditions observed by Taylor *et al.* (2014). The sand is a washed, poorly graded, medium-to-fine quartz-silica beach sand with 90% of the material between 0.25 and 0.85 mm in diameter, similar to the material within the region presented in Taylor *et al.* (2014). The coefficient of uniformity and coefficient of curvature of the grain-sized distribution are 1.52 and 1.12, respectively. The specific gravity is 2.67.

3.3 Sample saturation for comparison to field conditions

To replicate field conditions observed by Taylor *et al.* (2014) the drainage valve was set to a free-draining condition, that is the permeability at the sample base was greater than the permeability of the soil sample. The maximum saturation was achieved via a dynamic flow, that is a continuous rain event, until a steady-state condition was achieved wherein the inflow was equal to the outflow through the specimen. At the point of maximum saturation, no further absorption will occur. After a steady-state condition was achieved, the inflow of water was ceased and the specimen was allowed to freely drain through the sample base and evaporate through the atmospheric free-surface boundary interface. The drying process was accelerated with the aid of a small electric heater placed near the specimen. Care was taken so that the specimen was not subjected to direct exterior forces (e.g. vibrations and forced air), as artificial particle reorientation would render the subsequent data invalid. For the replication of field conditions, a single wetting/drying cycle was conducted over 3 months on a vibratory isolation table under controlled ambient conditions: 21°C at a relative humidity between 55% and 60%.

3.4 Controlled sample saturation for soil fabric studies

To investigate the changes in the soil fabric or structure at discrete controlled saturation intervals, the drainage valve was set to an impervious condition, that is no flow was allowed through the specimen. Controlled saturation was achieved by
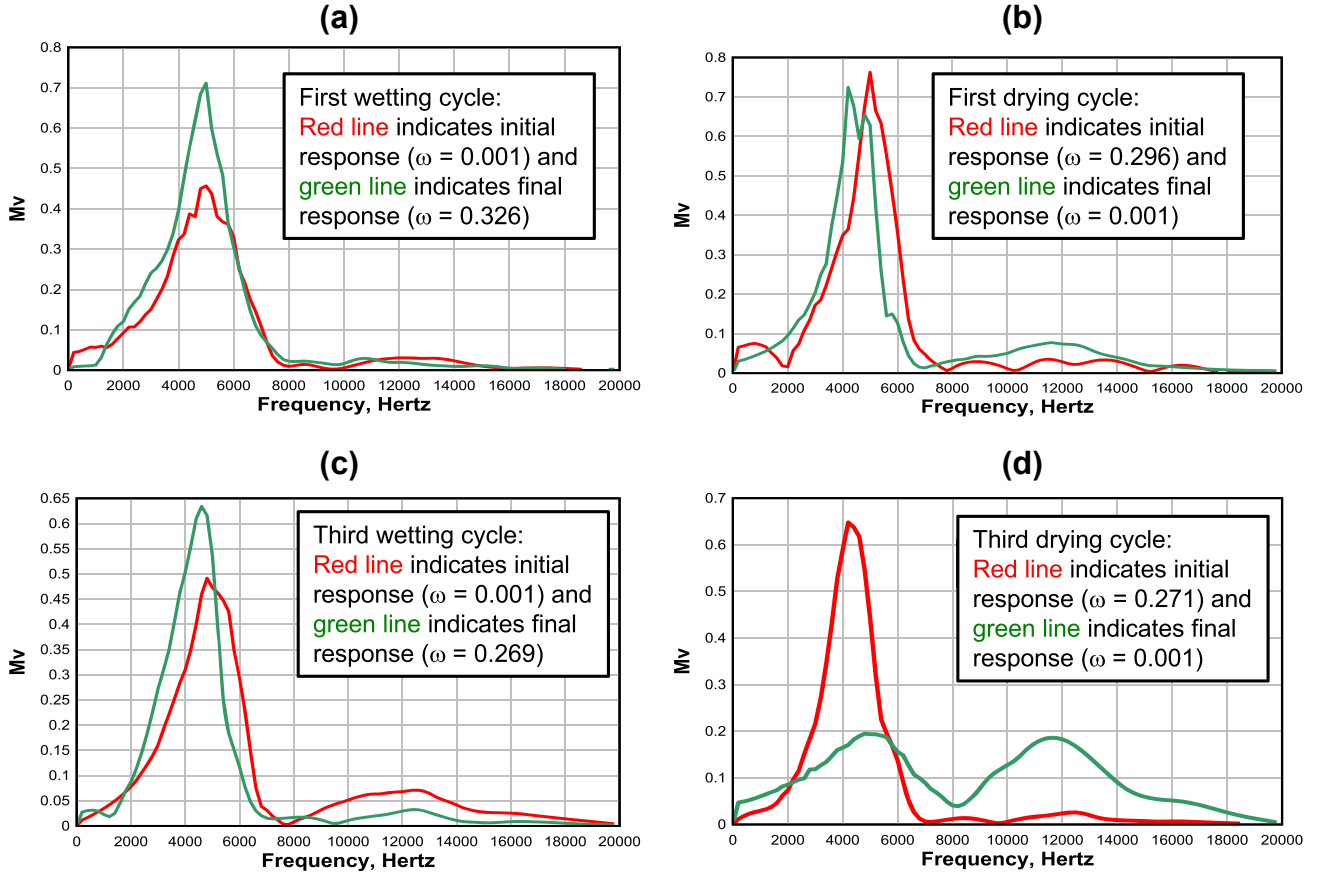
Figure 2 Horizontally propagating FFT response, measured in millivolts (mV), observed in Tip-to-Tip source function tests subjected to a 10-kHz, 0.1-ms, 14-volt sine wave driver. (a) First wetting cycle; (b) first drying cycle; (c) third wetting cycle; and (d) third drying cycle on the same specimen.

adding 70 mL of water, via a pipette, to the specimen over a 5-minute period. The specimen was then covered with plastic wrap to prevent evaporation, and allowed to reach a hydraulic equilibrium, determined by no additional change in the pore pressure transducers. The amount of time required to reach hydraulic equilibrium is a function of the soil composition and the sample preparation. Four hours was required for this study. After hydraulic equilibrium was achieved, a measurement of compressional and shear waves, p- and s-waves, respectively, were taken for the known degree of saturation. This process was repeated until no further absorption of the water occurred and hydraulic equilibrium was maintained; this was determined to be the maximum saturation achievable by the soil without the use of applied external pressures that do not occur under field conditions. Once the specimen achieved maximum saturation, the specimen was allowed to dry while continuing to take moisture and wave speed measurements intermittently as the specimen dried. A single wetting/drying cy-

cle was conducted over a 3-month timeframe under controlled ambient conditions: 21°C at a relative humidity between 55% and 60%.

3.5 Determination of an accurate source function with respect to saturation

In order to numerically model wave behaviour within the ultrasonic near-surface inundation testing device, an accurate source function is required as the soil-bender element coupling is a function of the saturation within the soil fabric. The internal source function of a bender element is a pure sine wave; however, the peizoeletric element couples with the soil structure and is susceptible to saturation coupling effects. Therefore, tip-to-tip source testing was used as a baseline to determine how the bender element source input functioned during wetting and drying cycles. The bender elements were placed with the transmitter and the receiver parallel in the centre of

the specimen at a spacing of less than 1 mm. The tip-to-tip results over the initial wetting cycle (Fig. 2a, starting at an initial dry gravimetric water content, $\omega = 0.001$, and wetted to a final gravimetric water content, $\omega = 0.326$) indicate that the source function varies with saturation with a higher frequency amplitude response when saturated. The higher response amplitude was observed over all wetting and drying cycles, Fig. 2. A hysteretic effect was observed in the functional form of the produced source over multiple wetting/drying cycles. However, this hysteretic behaviour was not uniform over the number of cycles tested, for example the final drying response in the third drying cycle (green line in Fig. 2d) is functionally different than the final drying response of the first drying cycle (green line in Fig. 2b). Therefore, numerical model analyses require that the source function must be a measured laboratory value as a function of saturation and wetting/drying cycle and should not be simply assumed uniform.

3.6 Direct measurement of wave speeds

The use of piezoelectric bender elements has been used for decades in geotechnical laboratory testing (Shirley 1978; Bates 1989; Brignoli, Gotti and Stokoe 1996; Arulnathan, Boulanger and Riemer 1998; Pennington, Nash and Lings 2001; Lee and Santamarina 2005; Leong, Yeo and Rahardjo 2005; Viana da Fonseca, Ferreira and Fahey 2009; Gu, Yang and Huang 2013). The uncertainties within the data can be traced to the method of interpretation used to determine the wave travel time. Proper methods for picking wave arrivals using bender elements have been studied extensively for several decades (e.g. Arulnathan *et al.* 1998; Lee and Santamarina 2005; Leong *et al.* 2005; Viana da Fonseca *et al.* 2009). The shear wave arrival was determined through cross-correlation (Viana da Fonseca *et al.* 2009) and manual inspection to determine the correct travel time. The p-wave was excluded from the cross-correlation by identifying the end of the p-wave in the time-series and performing the cross-correlation on the signal only after that time. During inundation, the results indicated a decrease in s-wave amplitude wherein the cross-correlation method did not work even when an s-wave could be visually identified, which was indicative of significant changes to wave energy and spectral phase content. Therefore, the two methods must be used in conjunction to determine the correct wave arrival and interpret the change in spectral content as observed in Taylor *et al.* (2014).

The ratio of the transmitted signal wavelength to the bender element's length (λ/l_b) greatly affected accuracy of the travel time for a given sample as well as the signal-to-noise

ratio (SNR) defined as (Carlson 1986; Arulnathan *et al.* 1998; Leong *et al.* 2005; Viana da Fonseca *et al.* 2009):

$$\text{SNR} = 10 \log \frac{\text{Signal power}}{\text{Noise power}}, \tag{1}$$

where the noise and signal power can be obtained from the power or frequency spectrum of the receiver signal. An SNR of at least 4 dB is required for wave speed measurements (Leong *et al.* 2005). The transmission frequency of 10 kHz was chosen to maximize the travel time accuracy while reducing near-field effects (Leong *et al.* 2005). The wave path length to wavelength ratio must be a minimum of 3.33 per Leong *et al.* (2005); for this study, the minimum wave path to wavelength ratio is 3.40 for the fastest p-wave velocity. A minimum of 50 stacked waveforms were used at each data interval to determine the propagated signal. Propagation testing within the ultrasonic near-surface inundation testing device can investigate wave propagation horizontally and vertically (both with and against fluid flow). The orientation of the bender elements was dependent on the desired motion to be investigated; parallel elements for radial motion and perpendicular for translational motion. To minimize the noise associated with dynamic fluid flow and investigate soil fabric effects, the horizontal radial motion bender element orientation is presented herein.

4 RESULTS

4.1 Soil fabric effects: compressional wave velocity

The shear wave response correlates to the soil structure or fabric and is of principle interest for geotechnical engineering and soil behavioural characteristics. However, within the near surface, the p-wave and s-wave response are equally critical for research with respect to detection, classification and localization signal processing schemes. The p-wave velocity, v_p, of the soil is usually treated as effective solid continuum and expressed as

$$v_p = \sqrt{\frac{K + \frac{4}{3}G}{\rho}}, \tag{2}$$

where K is the bulk modulus, G is the shear modulus and ρ is the bulk density. However, K and G are functionally dependent on the degree of saturation, the fabric or structure of the soil, and require *a priori* knowledge of the saturation impacts on the granular contacts and stiffness matrix (Cho and Santamarina 2001; Fratta *et al.* 2005; Taylor *et al.* 2014). The characteristic soil behaviour, outside of the residual and saturated regions, is assumed to be governed by the soil's
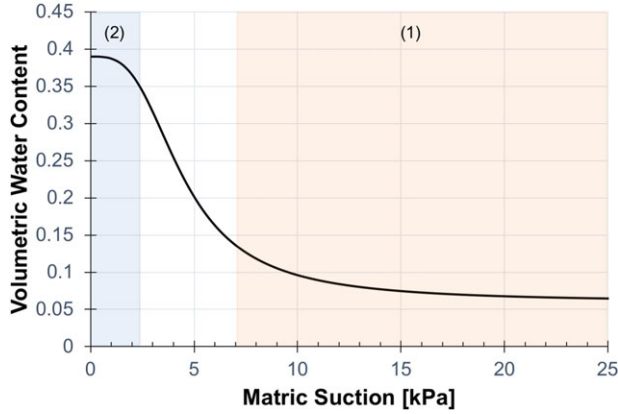
Figure 3 Soil-water retention curve after Walshire *et al.* (2017). (1) The residual region; (2) saturated region.

matric suction defined by the soil-water characteristic curve (SWCC), soil-water retention curve (SWRC), or more broadly the suction-water content relationship (SWR) (Fredlund 2002; Fratta *et al.* 2005; Lu and Likos 2006; Lu and Sabatier 2009; Lu *et al.* 2010; Fredlund *et al.* 2012; Malaya and Sreedeep 2012; Han and Vanapalli 2016; Muraleetharan, Hoyos and Ge 2016). Therefore, it is assumed that the v_p response should follow a similar trend, that is functional expression, to that of the soil matric suction. Walshire *et al.* (2017) performed a detailed laboratory investigation on the matric suction potential of this material with the data fit using the van Genuchten (1980) numerical model, expressed as

$$\theta = \theta_r + \frac{(\theta_s - \theta_r)}{[1 + (\alpha \psi)^n]^{1/1-n}}, \tag{3}$$

Table 1 UNIT v_p-saturation and v_s-saturation data from controlled sample saturation

	Original Identifier	Gravimetric Saturation	P-Wave Velocity (m/s)	S-Wave Velocity (m/s)
First static infiltration cycle	Cube2_stat_70ml_3_P-wave	0.09	269	131
	Cube2_stat_140ml_3_P-wave	0.10	287	134
	Cube2_stat_210ml_3_P-wave	0.16	282	127
	Cube2_stat_280ml_3_P-wave	0.21	326	127
	Cube2_stat_350ml_3_P-wave	0.27	368	113
	Cube2_stat_420ml_3_P-wave	0.31	378	111
	Cube2_stat_560ml_3_P-wave	0.42	385	110
	Cube2_stat_630ml_3_P-wave	0.53	413	110
	Cube2_stat_700ml_3_P-wave	0.62	411	110
	Cube2_stat_770ml_3_P-wave	0.69	425	107
	Cube2_stat_838ml_3_P-wave	0.70	426	104
First static drying cycle	Cube2_stat_4-4-18_P-wave	0.65	421	109
	Cube2_stat_4-5-18_P-wave	0.52	413	111
	Cube2_stat_4-6-18_P-wave	0.36	382	113
	Cube2_stat_4-10-18_P-wave	0.25	349	119
	Cube2_stat_4-12-18_P-wave	0.18	285	119
	Cube2_stat_4-13-18_P-wave	0.17	285	126
	Cube2_stat_4-18-18_P-wave	0.16	286	128
	Cube2_stat_4-20-18_P-wave	0.13	261	136
	Cube2_stat_4-24-18_P-wave	0.12	260	139
	Cube2_stat_4-26-18_P-wave	0.07	260	139
Second static infiltration cycle	Cube2_stat_70ml_4_P-wave	0.08	262	134
	Cube2_stat_140ml_4_P-wave	0.24	289	118
	Cube2_stat_210ml_4_P-wave	0.28	353	112
	Cube2_stat_280ml_4_P-wave	0.30	362	118
	Cube2_stat_350ml_4_P-wave	0.32	389	118
	Cube2_stat_420ml_4_P-wave	0.34	408	116
	Cube2_stat_490ml_4_P-wave	0.38	421	114
	Cube2_stat_560ml_4_P-wave	0.43	423	111
	Cube2_stat_630ml_4_P-wave	0.55	433	105
	Cube2_stat_700ml_3_P-wave	0.66	425	114
	Cube2_stat_770ml_3_P-wave	0.69	425	100
	Cube2_stat_827.2ml_3_P-wave	0.70	420	108
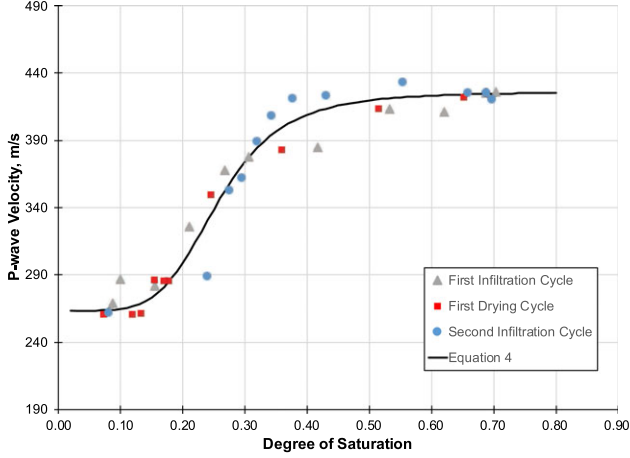
Figure 4 Relationship of p-wave velocity to saturation from controlled sample saturation.

where θ, θ_r and θ_s are the volumetric water content, the residual volumetric water content (0.06) and saturated water content (0.39), respectively. Note that α (in units of 1/pressure; 0.26 in this study) and n are curve-fitting parameters related to the pore size distribution (3.29 in this study), and ψ is the matric suction. The SWRC for this material is shown in Fig. 3, from Taylor *et al.* (2019).

The ultrasonic near-surface inundation testing (UNIT) v_p data, Table 1 and Fig. 4, follows the same functional relationship to equation (3) and Fig. 3, where the v_p is unchanged within the residual (dry) and saturated regions. Thus, the relationship between v_p and the degree of saturation, S, was fit
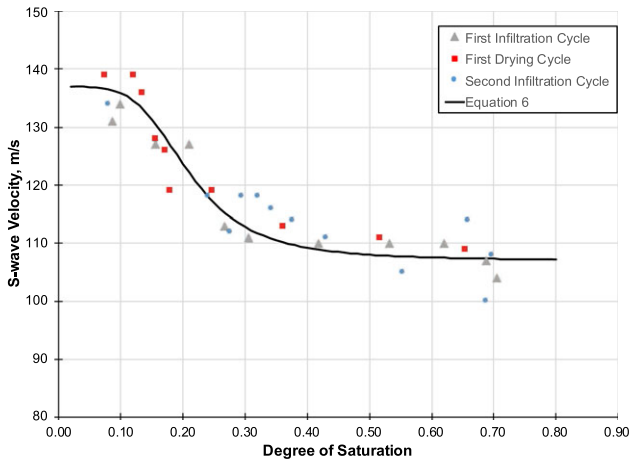
numerically based on a modified form of the van Genuchten (1980) matric suction relationship as

$$v_p = v_p^s + \frac{v_p^r - v_p^s}{[1 + (\alpha S)^n]^{(m)}},\tag{4}$$

where v_p^s is the p-wave velocity corresponding to the saturated state (i.e. 426 m/s for degree of saturation greater than 70%), v_p^r is the p-wave velocity corresponding to the residual condition where a soil's matric suction does not contribute to the behaviour of the soil element (i.e. 264 m/s that corresponds to residual saturation ($S < 13\%$) for this soil) and α, m and n are empirical curve fitting parameters (i.e. 4.0, 0.9 and 5.15, respectively, in this study). Unlike semi-theoretical models (e.g. Fratta *et al.* 2005), equation (4) implicitly accounts for all microscopic (i.e. granular level) variability in actual moduli behaviour with saturation.

Both field and laboratory investigations indicate the potential for correlation of v_p to the degree of saturation (Tsukamoto *et al.* 2002; Yang 2002; Takahashi *et al.* 2006). However, other research has shown that using the v_p to determine fully saturated conditions is not reliable (Ishihara, Huang and Tsuchiya 1998; Tamura *et al.* 2002; Naesgaard, Byrne and Wijewckreme 2007). The results of the UNIT testing illustrate that while a v_p-saturation relationship, equation (4), does exist, the material exhibits a sharp increase in v_p with the degree of saturation between 20% and 40% with little change outside this range, irrespective of wetting or drying cycles, Fig. 4. Therefore, using v_p as an indicator for the degree of saturation is only accurate within the 20–40% saturation region and should not be used to determine if a soil is in a fully saturated condition.

4.2 Soil fabric effects: shear wave velocity

Small strain properties of soil, that is shear modulus, Young's modulus, bulk modulus, constrained modulus and Poisson's ratio, are critical in understanding and modelling many geotechnical and geophysical problems (Fratta *et al.* 2005; Barriere *et al.* 2012). The shear wave velocity, v_s, is typically used as a measure of the soil structure or fabric and typically defines the shear modulus, G, as

$$G = \left[\bar{p} + \frac{p^* p_A}{p^* + p_A} \right] v_s^2,\tag{5}$$

where $\bar{p}$ is the mass density of the elastic media, p^* is the mass density of the fluid, and p_A is the mass density of the additional mass in relation to the fluid-structure coupling. For a saturated soil, the total density can be substituted in the
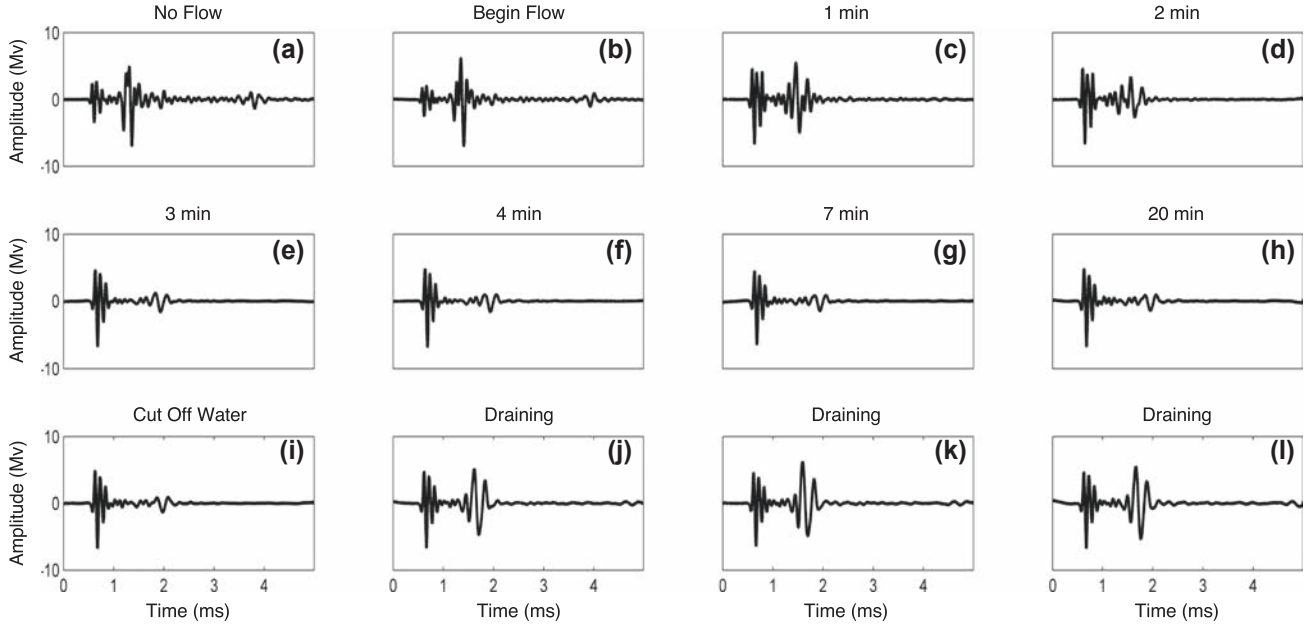

Figure 5 Relationship of s-wave velocity to saturation from controlled sample saturation.

Figure 6 Horizontally propagating time-history for a single dynamic wetting/drying cycle. Panels A–D and J–L have an identifiable s-wave. Panels E–I do not have identifiable s-waves.

denominator as a first-order approximation of the shear wave velocity but p_A varies with both permeability and grain size.

The ultrasonic near-surface inundation testing v_s data, Table 1 and Fig. 5, follows the same functional relationship to equation (4) and Fig. 3, where the v_s is unchanged within the residual (dry) and saturated regions. As v_s is typically used as a measure of soil fabric stiffness, it has the same dependency as v_p with matric suction thus, the relationship between v_s and the degree of saturation, S, was fit numerically as

$$v_s = v_s^s + \frac{v_s^r - v_s^s}{[1 + (\alpha S)^n]^{(m)}}, \tag{6}$$

where v_s^s is the shear wave velocity corresponding to the saturated state (i.e. 107 m/s for degree of saturation greater than 70%), v_s^r is the shear wave velocity corresponding to the residual condition where a soil's matric suction does not contribute to the behaviour of the soil element (i.e. 137 m/s that corresponds to residual saturation ($S < 13\%$) for this soil) and α, m and n are empirical curve fitting parameters (i.e. 5.1, 0.8 and 4.5, respectively, in this study).

Unlike Fig. 4, the variation in shear wave magnitude with degree of saturation is significantly smaller with the v_s decreasing with increasing saturation. During dynamic flow, that is simulated rain events, it was observed that v_s amplitude decreased to less than the signal noise and was therefore undetectable when the specimen achieved a steady state flow condition, the point of maximum degree of saturation (72–

79%), Fig. 6. This observed response is in keeping with field observations by Taylor *et al.* (2014). Once the influx of water ceased and the degree of saturation decreased to below 72% the v_s could be identified, Fig. 6. The combination of a damped v_s amplitude and a maximum degree of saturation of 72–79% suggests that during the wetting process the soil passes through the suction failure plane, that is the matric suction is insufficient to provide enough tensile strength to maintain a continuum within the grains without an increase in external confinement. Thus, the specimen should no longer be represented as a continuum, but rather as failed mass or viscoelastic material. This conclusion is further supported by self-supporting unconfined drained triaxial testing presented by Taylor *et al.* (2019), wherein suction failure is observed between 70.5% and 76.5% saturation with the specimen behaving as a viscoelastic media during failure.

4.3 General waveform observations

A modified, discrete Fast Fourier Transform (FFT) is utilized to investigate the wetting and drying cycles in frequency space of the detrended data (Smart and Flinn 1971; Swarztrauber 1982; Press *et al.* 1986). The discrete modified FFT is used specifically to incorporate the entire time history without having to pad, filter or apply a window to the data before transforming the time domain into the frequency domain
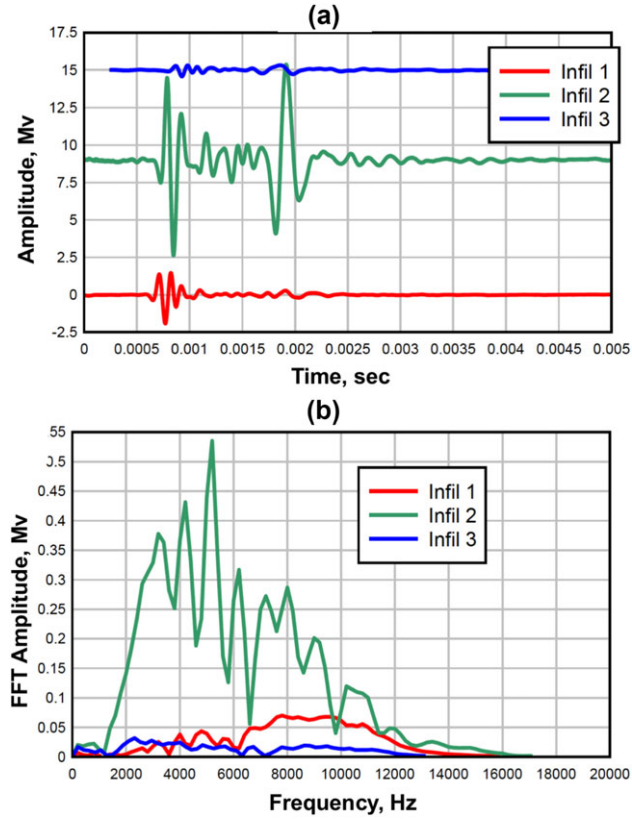
Figure 7 Horizontally propagating time histories and FFT response for three wetting cycles on the same specimen. The wetting cycle starts at a residual (dry) moisture content and is then saturated until no additional fluid is absorbed by the soil fabric. The data are the final saturation condition for each wetting cycle.

Figure 8 Horizontally propagating time histories and FFT response for four drying cycles on the same specimen as Fig. 7. The drying cycle begins at the saturated state and dried until a residual (dry) moisture content is measured. The data are the residual (dry) state for each drying cycle.

(Swarztrauber 1982). The FFT response and time histories of the propagated source, Figs 7 and 8, indicate an untrended variability for both wetting and drying cycles, respectively. The time histories, Figs 7(a) and 8(a), suggest that the shear wave can arrive sooner or later than the previous cycle state, implying that the soil fabric is not static, despite there not being any measurable volumetric changes during testing. In the FFT space, similar characteristic changes can be observed both in tip-to-tip source testing, Fig. 2, and in propagation testing, Figs 7(b) and 8(b); however, these similarities are not observed at the same number of wetting and drying cycles. For example, the double peak FFT response, Fig. 2(d), is observed in the third drying cycle in tip-to-tip testing but in the fourth drying cycle in the propagation testing, Fig. 8(b). This change in wave characteristics suggests a stochastic change in fabric structure after each cycle; thus, the assumption of constant or discrete values of moduli, porosity, Poisson's ratio and associated density are not universally valid for all satu-
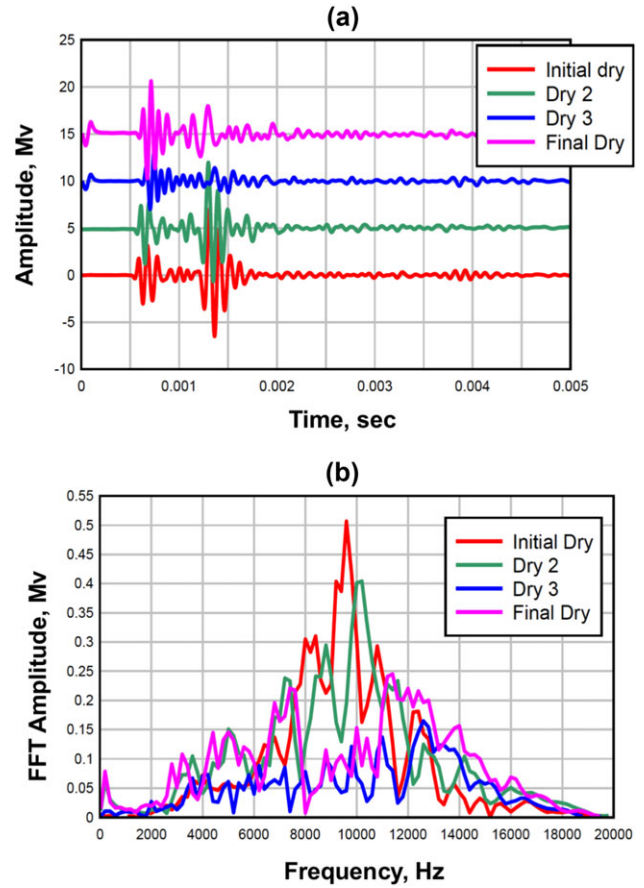
ration conditions. Rather, each discrete degree of saturation will have a distribution of wave characteristics, moduli and wave speeds and the behaviour at any such discrete interval should be obtained via a probabilistic numerical simulation. These distributions are beyond the scope of this paper and the subject of ongoing research.

Table 2 Comparison of Taylor *et al.*(2014) field data and UNIT v_p and v_s measurements

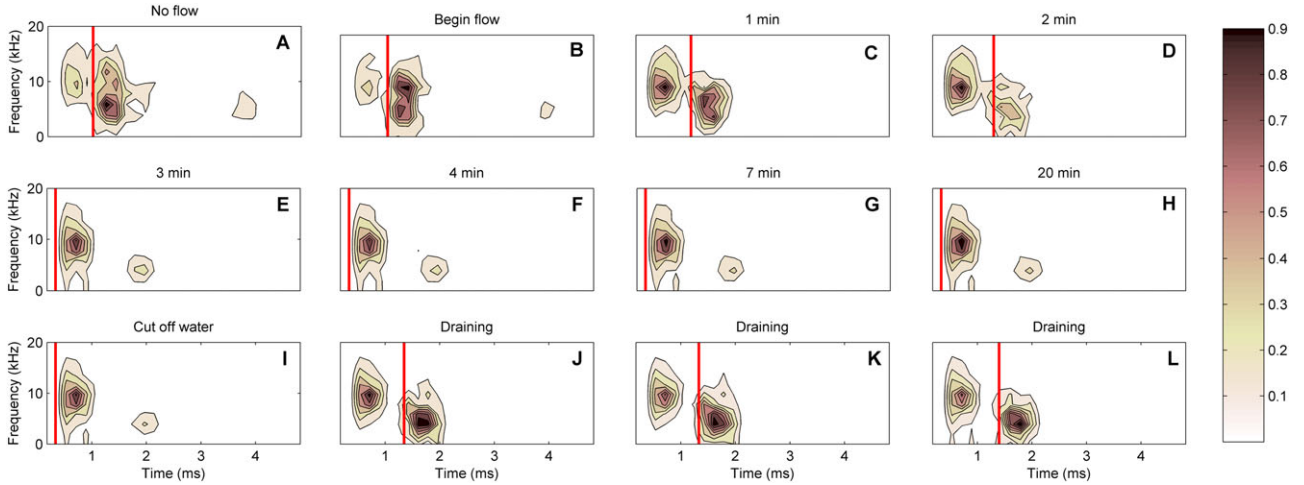| | Taylor *et al.* (2014) | | UNIT Data | |
	pre-rain	post-rain	residual saturation	25% saturation
v_p	284 m/s	333 m/s	280 m/s	339 m/s
v_s	138 m/s	155 m/s	137 m/s	120 m/s

Figure 9 Relative power spectral density response for the single dynamic wetting/drying time-histories shown in Fig. 6. Panels A–D and J–L have an identifiable s-wave. Panels E–I do not have identifiable s-waves.
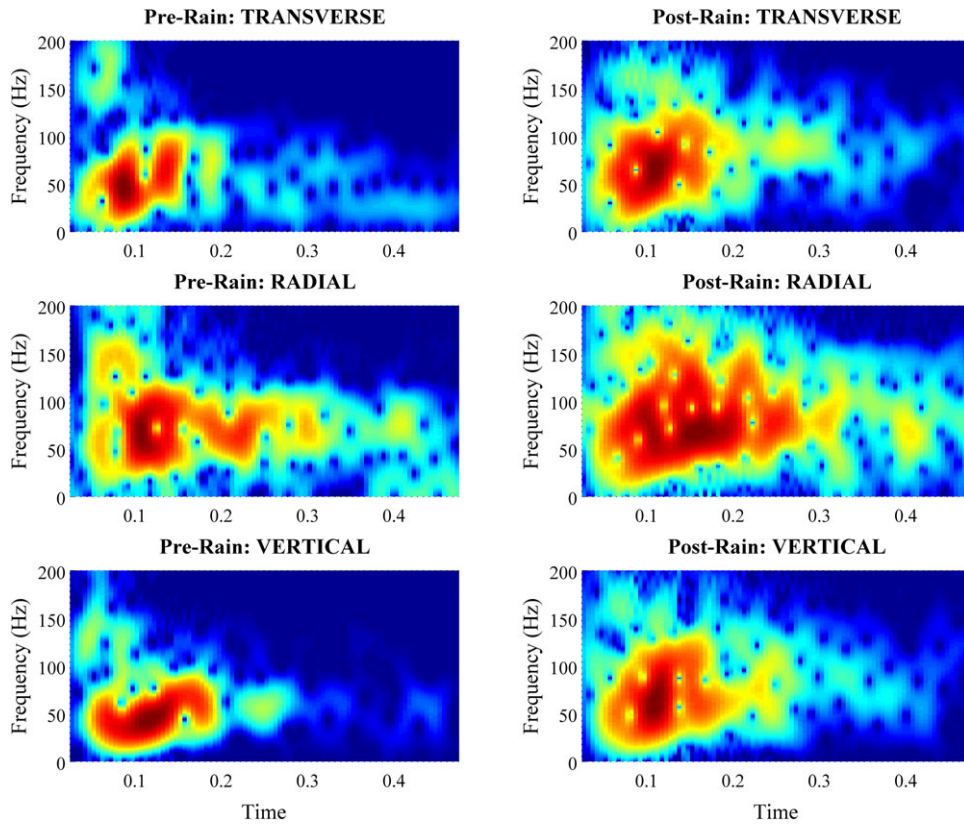

Figure 10 Relative power spectral density of the field geophone response pre- and post-rain event (from Taylor *et al.* 2014).

4.4 Comparison of the UNIT data to field observations

Taylor *et al.* (2014) noted significant variability within the pre- and post-rain waveforms generated from the same source. Using the radial axis, the ultrasonic near-surface inundation test-

ing (UNIT) data was compared to the field geophone response to see if the UNIT accurately reflected the filed phenomenology. The radial axis was used as it is the weakest principle axis within the soil which would be the most sensitive to structural changes within the soil fabric. An initial comparison of the v_s

and v_p pre-rain velocities were made with the residual region, $S < 13\%$, within the UNIT, Table 2. The pre-rain and UNIT v_p and v_s measurements were in good agreement with the dry field condition from Taylor *et al.* (2014). Due to the operational nature of the data collection by Taylor *et al.* (2014), no discrete field saturation or soil sample was obtained. From the v_p field data, 333 m/s, a correlation was made via the UNIT v_p data, equation (4), to determine the approximate degree of saturation post-rain of approximately 25%. The resulting UNIT and field v_s differ by 26 m/s, due to the use of a proxy physical field sample in conjunction with a distribution of possible v_s values, the phenomenology recreation was further correlated via amplification of the received signal. Taylor *et al.* (2014) observed a 4.6-fold increase in the maximum absolute radial post-rain velocity. Comparing the average UNIT bender element received signal voltage output for all v_p in the residual region (less than 15% gravimetric saturation) and the average voltage for gravimetric saturations between 21% and 28%, there was an average signal amplification of 1.6-fold similar to the v_p amplitude increase from Taylor *et al.* (2014).

Taylor *et al.* (2014) also noted that there was a significant shift in dominant frequency between pre- and post-rain events. While the UNIT and field sources vary significantly in frequency content, the relative power spectral densities were compared for similarities in shape with increased moisture. Figure 9 shows that within the UNIT a similar decreasing shift in dominant frequency occurred between the residual (Panel A) and draining conditions (Panels J–L) similar to the frequency decrease observed in the radial geophones from Taylor *et al.* (2014), Fig. 10. It should be noted that as water is flowing into the sample (Panels B–H), the dominant frequency increases significantly compared to the residual condition (Panel A).

5 CONCLUSIONS

Although it will never be ideal to install seismic sensors in near-surface soil, less than 1m of overburden, the operational necessity of doing so for rapidly deployable, semi-permanent seismic arrays dictates that this can no longer be a neglected field of research in order to ensure accurate detection, classification and localization of seismic events utilizing the meteorologically sensitive p-wave and shear wave portions of the wavefield. Field data from Taylor *et al.* (2014) illustrated a significant signal amplitude increase, change in frequency content with no change in signal duration before and after 36 hours of steady precipitation. Laboratory replication of

these phenomena has never before been demonstrated due to the lack of appropriate equipment.

A new Ultrasonic Near-surface Inundation Testing (UNIT) device is presented as a means to study the effects of moisture and inundation within the near-surface environment where confining pressures are negligible and wave propagation is greatly influenced by the soil structure and saturation. The data presented here adequately replicates field observations of shallow-buried geophysical sensors during meteorological events and identifies important wave behavioural characteristics for future flow experimentation, sensor processing and system performance optimization. Additionally, the development of new v_p-saturation and v_s-saturation relationships as a function of the matric suction of the soil indicates that the UNIT device can be used to investigate seismic propagation under active inundation conditions and for the derivation of appropriate moduli.

REFERENCES

Arulnathan R., Boulanger R. and Riemer M. 1998. Analysis of bender element tests. *Geotechnical Testing Journal* **21**, 120–131.

Bachrach R. and Nur A. 1998a. High-resolution shallow-seismic experiments in sand, part 1: water table, fluid flow, and saturation. *Geophysics* **63**, 1225–1233.

Bachrach R. and Nur A. 1998b. High-resolution shallow-seismic experiments in sand, part 1: velocities in shallow unconsolidated sand. *Geophysics* **63**, 1234–1240.

Bachrach R., Dvorkin J. and Nur A. 2000. Seismic velocities and Poisson's ratio of shallow unconsolidated sands. *Geophysics* **65**, 559–564.

Barriere J., Bordes C., Brito D., Senechal P. and Perroud H. 2012. Laboratory monitoring of P waves in partially saturated sand. *Geophysical Journal International* **191**, 1152–1170.

Bates C.R. 1989. Dynamic soil property measurements during triaxial testing. *Geotechnique* **39**, 721–726.

Bergamo P., Dashwood B., Uhlemann S., Swift R., Chambers J., Gunn D., *et al.* 2016a. Time-lapse monitoring of climate effects on earthworks using surface waves. *Geophysics* **81**, EN1–EN15.

Bergamo P., Dashwood B., Uhlemann S., Swift R., Chambers J., Gunn D., *et al.* 2016b. Time-lapse monitoring of fluid-induced geophysical property variations within an unstable earthwork using P-wave refraction. *Geophysics* **81**, EN17–EN27.

Biot M. 1956. Theory of elastic waves in a fluid-saturated porous solid. 1. Low frequency range. *The Journal of the Acoustical Society of America* **28**, 168–178.

Bishop A. and Blight G. 1963. Some aspects of effective stress in saturated and partly saturated soils. *Geotechnique* **13**, 177–196.

Bonner J., Waxler R., Gitterman Y. and Hofstetter R. 2013. Seismo-acoustic energy partitioning at near-source and local distances from the 2011 sayarim explosions in the Negev desert, Israel. *Bulletin of the Seismological Society of America* **103**, 741–758.

Brignoli E.G.M., Gotti M. and Stokoe K.H., II 1996. Measurement of shear waves in laboratory specimens by means of piezoelectric transducers. *Geotechnical Testing Journal* **19**, 384–397.

Carlson A.B. 1986. *Communication Systems—An Introduction to Signals and Noise in Electrical Communication.* McGraw-Hill, New York.

Chapman M. 2013. On the rupture process of the 23 august 2011 Virginia earthquake. *Bulletin of the Seismological Society of America* **103**, 613–628.

Cho G. and Santamarina J. 2001. Unsaturated particulate materials – particle-level studies. *Journal of Geotechnical and Geoenvironment Engineering* **127**, 84–96.

Cho G., Dodds J. and Santamarina J.C. 2006. Particle shape on packing density, stiffness, and strength: natural and crushed sands. *Journal of Geotechnical and Geoenvironment Engineering* **132**, 591–602.

Crane J., Lorenzo J. and Harris J. 2013. A new electrical and mechanical detonatable shear wave source for near surface (0-30 m) seismic acquisition. *Journal of Applied Geophysics* **91**, 1–8.

Fratta D., Alshibli K., Tanner W. and Roussel L. 2005. Combined TRD and P-wave velocity measurements for the determination of in situ soil density – experimental study. *Geotechnical Testing Journal* **28**, 553–563.

Fredlund D. 2002. Use of the soil-water characteristic curve in the implementation of unsaturated soil mechanics. *Proceedings of the Third International Conference on Unsaturated Soils*, Recife, Brazil, March 2002.

Fredlund D., Rahardjo H. and Fredlund M. 2012. *Unsaturated Soil Mechanics in Engineering Practice.* John Wiley & Sons.

Gassmann F. 1951. Uber die elastizitat poroser medien. *Veirteljahrsschrift der Naturforshenden Gesellshaft in Zurich* **96**, 1–23.

Gu X., Yang J. and Huang M. 2013. Laboratory measurements of small strain properties of dry sands by bender element. *Soils and Foundations* **53**, 735–745.

Han Z. and Vanapalli S. 2016. Stiffness and shear strength of unsaturated soils in relation to soil-water characteristic curve. *Geotechnique* **66**, 627–647.

Hasbrouck W. 1991. Four shallow-depth, shear-wave feasibility studies. *Geophysics* **56**, 1875–1885.

Hassanizadeh S., Celia M. and Dahle H. 2002. Dynamic effect in the capillary pressure-saturation relationship and its impacts on unsaturated flow. *Vadose Zone Journal* **1**, 38–57.

Houston S., Houston W. and Spadola D. 1988. Prediction of field collapse of soils due to wetting. *Journal of Geotechnical and Geoenvironment Engineering* **114**, 40–58.

Ishihara K., Huang Y. and Tsuchiya H. 1998. Liquefaction resistance of nearly saturated sand as correlated with longitudinal wave velocity. In: *Poromechanics: A tribute to Maurice A. Biot*, (eds J. Thimus, Y. Abousleiman, A. Cheng, O. Coussy and E. Detournay), pp. 583–586. Balkema, Rotter- dam, The Netherlands.

Jolly R. 1956. Investigation of shear waves. *Geophysics* **21**, 905–1110.

Koper K., Wallace T. and Aster R. 2003. Seismic recordings of the Carlsbad, New Mexico, pipeline explosion of 19 August 2000. *Bulletin of the Seismological Society of America* **93**, 1427–1432.

Lee J.-S. and Santamarina J. 2005. Bender elements: Performance and signal interpretation. *Journal of Geotechnical and Geoenvironment Engineering* **131**, 1063–1070.

Leong E., Yeo S. and Rahardjo H. 2005. Measuring shear wave velocity using bender elements. *Geotechnical Testing Journal* **28**, 488–498.

Lu N. and Likos W. 2006. Suction stress characteristic curve for unsaturated soil. *Journal of Geotechnical and Geoenvironment Engineering* **132**, 131–142.

Lu N., Godt J. and Wu D. 2010. A closed-form equation for effective stress in unsaturated soil. *Water Resources Research* **46**, W05515.

Lu Z. and Sabatier J. 2009. Effects of soil water potential and moisture content on sound speed. *Soil Science Society of America Journal* **73**, 1614–1625.

Malaya C. and Sreedeep S. 2012. Critical review on the parameters influencing soil-water characteristic curve. *Journal of Irrigation and Drainage Engineering* **138**, 55–62.

Miller R., Pullan S., Waldner J. and Haeni F. 1986. Field comparison of shallow seismic sources. *Geophysics* **51**, 2067–2092.

Miller R., Pullan S., Steeples D. and Hunter J. 1992. Field comparison of shallow seismic sources near Chino, California. *Geophysics* **57**, 693–709.

Muraleetharan K., Hoyos L. and Ge L. 2016. Special issue on experimental and computational geomechanics for unsaturated soils. *International Journal of Geomechanics* **16**, D2016001.

Naesgaard E., Byrne P. and Wijewckreme D. 2007. Is P-wave velocity an indicator of saturation in sand with viscous pore fluid? *International Journal of Geomechanics* **7**, 437–443.

Oelze M., O'Brien Jr., W. and Darmody R. 2002. Measurement of attenuation and speed of sound in soils. *Soil Science Society of America Journal* **66**, 788–796.

Pennington D.S., Nash D.F.T. and Lings M.L. 2001. Horizontally mounted bender elements for measuring anistropic shear moduli in triaxial clay specimens. *Geotechnical Testing Journal* **24**, 133–144.

Press W., Flannery B., Teukolsky S. and Vetterling W. 1986. *Numerical Recipes.* Cambridge University Press.

Santamarina J. 2001. Soil behavior at the microscale: particle forces. *Proceedings of a Symposium on Soil Behavior and Soft Ground Construction* in honor of Charles C. Ladd, Boston, MA, October 2001 pp. 1–32. MIT.

Shen J., Crane J., Lorenzo J. and White C. 2016. Seismic velocity prediction in shallow (30 m) partially saturated sand. *Journal of Environmental and Engineering Geophysics* **21**, 67–78.

Shirley D.J. 1978. An improved shear wave transducer. *Journal of Acoustic Society of America* **63**, 1643–1645.

Smart E. and Flinn E. 1971. Fast frequency-wavenumber analysis and fisher signal detection in real-time infrasonic array data processing. *Geophysical Journal International* **26**, 279–284.

Song A.J., West B.A., Taylor O.-D., O'Connor D., Parno M., Hodgdon T., *et al.* 2017. "Munition penetration-depth prediction" ERDC/CRREL TR-17-12. U.S. Army Engineer Research and Development Center, Hanover, NH.

Stump B., Pearson D. and Reinke R. 1999. Source comparisons between nuclear and chemical explosions detonated at rainier mesa, Nevada test site. *Bulletin of the Seismological Society of America* **89**, 409–422.

Sture S., Costes N., Batiste S., Lankton M., Al Shibli K., Jeremic B., *et al.* 1998. Mechanics of granular materials at low effective stresses. *Journal of Aerospace Engineering* **11**, 67–72.

Swarztrauber P. 1982. *Vectorizing the FFT's in Parallel Computations*. Academic Press.

Takahashi H., Kitazume M., Ishibasi S. and Yamawaki S. 2006. Evaluating the saturation of model ground by P-wave velocity and modeling of models for a liquefaction study. *International Journal of Physical Modelling in Geotechnics* **1**, 13–15.

Tamura S., Tokimatsu K., Abe A. and Sato M. 2002. Effects of air bubbles on B-value and P-wave velocity of a partly saturated sand. *Soils Found* **42**, 121–129.

Taylor O.-D. and Martin K. 2017. Ultrasonic near-surface inundation testing device. U.S. Patent 9,606,087-B1, issued March 28, 2017.

Taylor O.-D. and Winters K. 2017. Resonant column behavior of unsaturated near-surface sands. *Proceedings of the Second PAN American Conference on Unsaturated Soil Mechanics*, Dallas, TX, November 2017.

Taylor O.-D.S., McKenna M., Kelley J., Berry T., Quinn B. and McKenna J. 2014. Partially saturated soil causing variability in near surface seismic signals: a case history. *Near Surface Geophysics* **12**, 467–480.

Taylor O.S., Berry W., Winters K., Rowland W., Antwine M. and Cunningham A. 2017. Protocol for cohesionless sample preparation for physical experimentation. *Geotechnical Testing Journal* **40**, 284–301.

Taylor O.-D., Winters K., Berry W., Walshire L. and Kinnebrew P. 2019. Near-surface soils: self-supported unconfined drained sand specimens. *Canadian Geotechnical Journal* **56**, 307–319.

Tsoflias G., Steeples D., Czarnecki G., Sloan S. and Eslick R. 2006. Automatic deployment of a 2-D geophone array for efficient ultra-shallow seismic imaging. *Geophysical Research Letter* **33**, L09301.

Tsukamoto Y., Ishihara K., Nakazawa H., Kamada K. and Huang H. 2002. Resistance of partly saturated sand to liquefaction with reference to longitudinal and shear wave velocities. *Soils Found* **42**, 93–104.

Vanapalli S.K., Fredlund D.G., Pufahl D.E. and Clifton A.W. 1996. Model for the prediction of shear strength with respect to soil suction. *Canadian Geotechnical Journal* **33**(3), 379–392. https://doi.org/10.1139/t96-060.

van Genuchten M.T. 1980. A closed form equation predicting the hydraulic conductivity of unsaturated soils. *Soil Science Society of America Journal* **44**, 892–898.

Viana da Fonseca A., Ferreira C. and Fahey M. 2009. A framework interpreting bender element tests, combining time-domain and frequency domain methods. *Geotechnical Testing Journal* **32**, 1–17.

Walshire L.A., Taylor O.-D.S. and Berry W.W. 2017. "Testing Method and Fabric Effects on the SWCC of a Poorly Graded Sand." Proceedings of the Second PAN American Conference on Unsaturated Soil Mechanics, Dallas, TX, 2017.

Yang J. 2002. Liquefaction resistance of sand in relation to P-wave velocity. *Geotechnique* **52**, 295–298.

Yordkayhun S., Ivanova A., Giese R., Juhlin C., Cosma C. 2009. Comparison of surface seismic sources at the CO2SINK site, Ketzin, Germany. *Geophysical Prospecting* **57**, 125–139.

REPORT DOCUMENTATION PAGE

1. REPORT DATE *(DD-MM-YYYY)*	2. REPORT TYPE	3. DATES COVERED *(From - To)*
August 2021	Final	

4. TITLE AND SUBTITLE	5a. CONTRACT NUMBER
The Behaviour of Near-Surface Soils Through Ultrasonic Near-Surface Inundation Testing	5b. GRANT NUMBER
	5c. PROGRAM ELEMENT NUMBER

6. AUTHOR(S)	5d. PROJECT NUMBER
Oliver-Denzil S. Taylor, Amy L. Cunningham, Robert E. Walker, Mihan H. McKenna, Kathryn E. Martin, and Pamela G. Kinnebrew	5e. TASK NUMBER
	5f. WORK UNIT NUMBER

7. PERFORMING ORGANIZATION NAME(S) AND ADDRESS(ES)	8. PERFORMING ORGANIZATION REPORT NUMBER
Geotechnical and Structures Laboratory U.S. Army Engineer Research and Development Center 3909 Halls Ferry Road Vicksburg, MS 39180	ERDC/GSL MP-21-4

9. SPONSORING / MONITORING AGENCY NAME(S) AND ADDRESS(ES)	10. SPONSOR/MONITOR'S ACRONYM(S)
Assistant Secretary of the Army, Acquisition, Logistics and Technology (ASAALT) Washington, DC 20314	11. SPONSOR/MONITOR'S REPORT NUMBER(S)

12. DISTRIBUTION / AVAILABILITY STATEMENT

Approved for public release; distribution is unlimited.

13. SUPPLEMENTARY NOTES

14. ABSTRACT

Seismometers installed within the upper metre of the subsurface can experience significant variability in signal propagation and attenuation properties of observed arrivals due to meteorological events. For example, during rain events, both the time and frequency representations of observed seismic waveforms can be significantly altered, complicating potential automatic signal processing efforts. Historically, a lack of laboratory equipment to explicitly investigate the effects of active inundation on seismic wave properties in the near surface prevented recreation of the observed phenomena in a controlled environment. Presented herein is a new flow chamber designed specifically for near-surface seismic wave/fluid flow interaction phenomenology research, the ultrasonic near-surface inundation testing device and new v_p-saturation and v_s-saturation relationships due to the effects of matric suction on the soil fabric.

15. SUBJECT TERMS

Near surface, Seismic, S-wave, Soil, Velocity

16. SECURITY CLASSIFICATION OF:			17. LIMITATION OF ABSTRACT	18. NUMBER OF PAGES	19a. NAME OF RESPONSIBLE PERSON
a. REPORT	b. ABSTRACT	c. THIS PAGE	UU	19	19b. TELEPHONE NUMBER *(include area code)*
Unclassified	Unclassified	Unclassified			